Wegmüller U., T. Strozzi, and C. Werner, Ionospheric path delay estimation using split-beam interferometry,
Procs. IGARSS'2012, Munich, Germany, 22-27 July 2012

IONOSPHERIC PATH DELAY ESTIMATION USING SPLIT-BEAM INTERFEROMETRY

Urs Wegmüller, Tazio Strozzi, and Charles Werner

Gamma Remote Sensing, CH-3073 Gümligen, Switzerland
http://www.gamma-rs.ch, E-Mail: wegmuller@gamma-rs.ch

ABSTRACT

Azimuth spectrum band-pass filtering has been applied successfully for estimation of along-track ground displacement [1] as well as for other applications, such as the identification of directional scattering [2] and the coherence estimation for long-baseline pairs [3]. Particularly L-band split-beam interferograms have shown another phase component related to along-track variations in the ionospheric path delay. In our work we present methodologies to identify and quantify ionospheric path delays affecting an interferogram using the corresponding split-beam interferogram.

Index Terms— *Split-beam interferometry, ionosphere, ionospheric path delay*

1. INTRODUCTION

Free electrons in the ionosphere interact with electromagnetic waves as a dispersive medium, with inverse effects on the phase and group velocities with stronger effects at lower frequencies. Meyer et al. [1] summarized the theoretical background of ionospheric propagation and evaluated the possibility of measuring ionospheric electron concentrations using a pair of SAR acquisitions, mainly concentrating on interferometric range phase gradients and range registration offsets. In our previous work on this subject [2] we presented a method to detect ionospheric anomalies in a single SAR acquisition to operationally check L-band SAR data for ionospheric anomalies. Anomalous azimuth offsets between pairs of repeat-orbit acquisitions are another clear indication for the presence of ionospheric effects. A modified offset tracking method, separating ground motion and ionosphere related offsets was presented and successfully applied. The estimated offset fields were also used to significantly improve the coherence of interferograms in the case of ionospheric anomalies. Finally, the observed ionospheric effects were also used to address the possibility of mapping electron concentration densities. Information on the location, altitude, and relative electron density change can be derived.

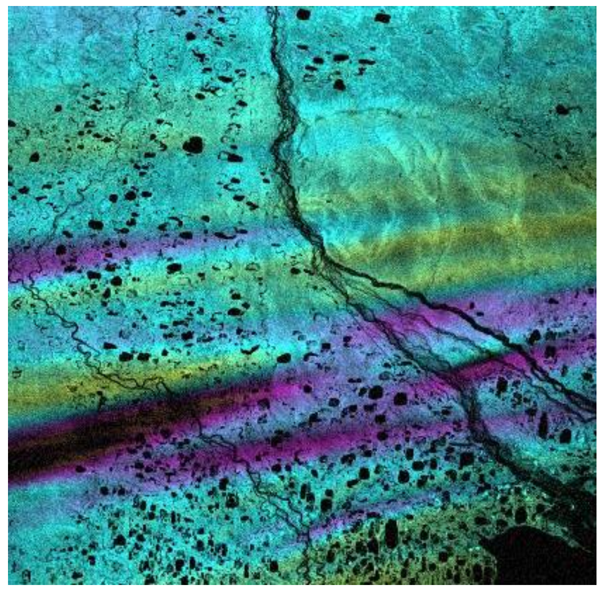

Figure 1 PALSAR multi-look split-beam interferogram of an area in Alaska. One color cycle corresponds to one 2π phase cycle. Image shown is in slant range geometry and corresponds to a full frame.

The objective of our present work is the identification and estimation of the ionospheric path delay affecting an interferogram using the corresponding split-beam interferogram. Azimuth spectrum band-pass filtering has been applied successfully for estimation of along-track ground displacement [3] as well as for other applications, such as the identification of directional scattering [4] and the coherence estimation for long-baseline pairs [5]. Particularly L-band split-beam interferograms have shown another phase component related to along-track variations in the ionospheric path delay. An example is shown in Figure 1.

An important reason to use split-beam interferograms instead of azimuth offset fields is that we can calculate the split-beam interferogram much more efficiently than the corresponding azimuth offset field with similar spatial sampling. In our contribution we discuss the processing methodology, discuss related challenges and show results.

2. METHODOLOGY

2.1. Split-beam interferogram

The main steps used to calculate a split-beam interferogram are co-registration of a pair of SLCs, azimuth spectrum band-bass filtering, calculation of the sub-band interferograms, and combining the sub-band interferograms into the split-beam interferogram. Some aspects need to be considered in more detail. Gradients of the ionospheric phase delay within a synthetic aperture introduces significant azimuth positional offsets. In SAR interferometry co-registration errors lead to interferometric decorrelation. In our method [6] we first estimate a registration offset field based on the orbital data and the terrain topography. A large area correction to this accounts for inaccuracies in the orbit geometry. This correction consists of first order polynomials in range and azimuth. Using these offsets the two SLC images were co-registered. Deviations from this co-registration are related to surface displacements and ionospheric azimuth offsets. Next, the ionospheric azimuth offsets are determined and added to the previously measured offset field. The slave SLC is then transformed in a single resampling step to the geometry of the master SLC. The co-registered SLCs are then azimuth band-pass filtered with two band-pass filters covering different azimuth Doppler sub-bands to get two sets of azimuth sub-band SLCs. Only overlapping parts of the input azimuth spectra in the two SLCs are used. We then calculate single-look sub-band interferograms, combine these into a combined single-look interferogram that is then multi-looked. In this manner no terrain or orbital phases need to be estimated and subtracted. Spatial filtering is only done on the resulting multi-looked split-beam interferogram, if at all. The phase of the split-beam interferogram is the phase difference between the two sub-band interferograms.

Except for the along-track displacement phase the split-beam interferogram phase corresponds to the first derivative in azimuth direction of the ionospheric path delay phase.

2.2. Azimuth integration

Unwrapping and integrating the split-beam interferogram phase along the azimuth direction permits determining the ionospheric path delay phase for the corresponding normal interferogram. Two aspects are critical in this integration. The first one is that we have for each column an unknown integration constant. The second one is that we may have spatial gaps in the unwrapped phases, e.g. due to low coherence areas.

We have tried several approaches to determine the integration constants. The simplest assumption is to start from a constant path delay for a given image line. A more advanced assumption is to assume that the relative path delay is zero for each image column, which appears to be the better assumption than starting from a constant path delay at the first image line. Furthermore, we determined the exact scaling of the phase in the integration which depends on the separation of the azimuth sub-bands used.

In the case of gaps in the unwrapped phases we fill those using spatial interpolation. For this we consider the preferred orientation of the ionospheric anomalies to define the interpolator accordingly. Large gaps cannot be filled by interpolation, though, and therefore we are looking into developing a method that permits to adjust the integration constants based on the spatial neighborhood in range direction.

3. EXAMPLES

3.1. Checking Aquila Earthquake co-seismic pair for ionospheric effects

For a co-seismic PALSAR pair of the Aquila Earthquake on 6-April 2009 we calculated both the split-beam interferogram and the differential interferogram (Figure 2). The split-beam interferogram clearly indicates that no relevant ionospheric effects are present in the two acquisitions used. Consequently, it can be concluded that there is no significant effect of the ionosphere on the differential interferometric phase.

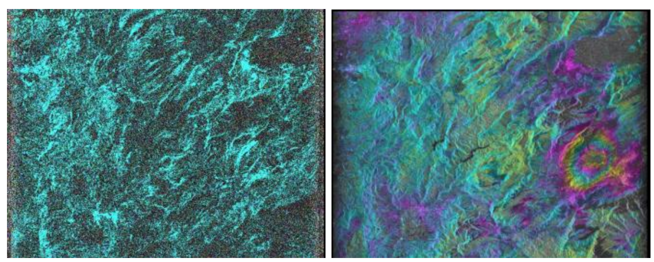

Figure 2 Aquila Earthquake, Italy. For the PALSAR pair 20080720 – 20090422 the split-beam interferogram (left) clearly indicates that the co-seismic interferometric phase (right) is not much affected by an ionospheric path delay. In both images one color cycle corresponds to one phase cycle. Image shown is in slant range geometry and corresponds to a full frame.

3.2. Checking PALSAR time series analysis over the Etna volcano for ionospheric effects

In the second example we used 19 PALSAR scenes to derive a displacement time series over the Etna Volcano in Italy. We defined a multi-reference stack including the pairs listed in Table 1 and calculated for each pair unwrapped differential interferometric phases. To check the presence of ionospheric effects we also calculated for each pair the split-beam interferogram (Figure 3). Overall the ionospheric effects are not very strong. Nevertheless, all pairs that include the scene acquired on 19-Jun-2009, consistently show strong ionospheric effects. As expected differential interferograms that include this scene also show strong phase variations (Figure 4).

Wegmüller U., T. Strozzi, and C. Werner, Ionospheric path delay estimation using split-beam interferometry,
Procs. IGARSS'2012, Munich, Germany, 22-27 July 2012

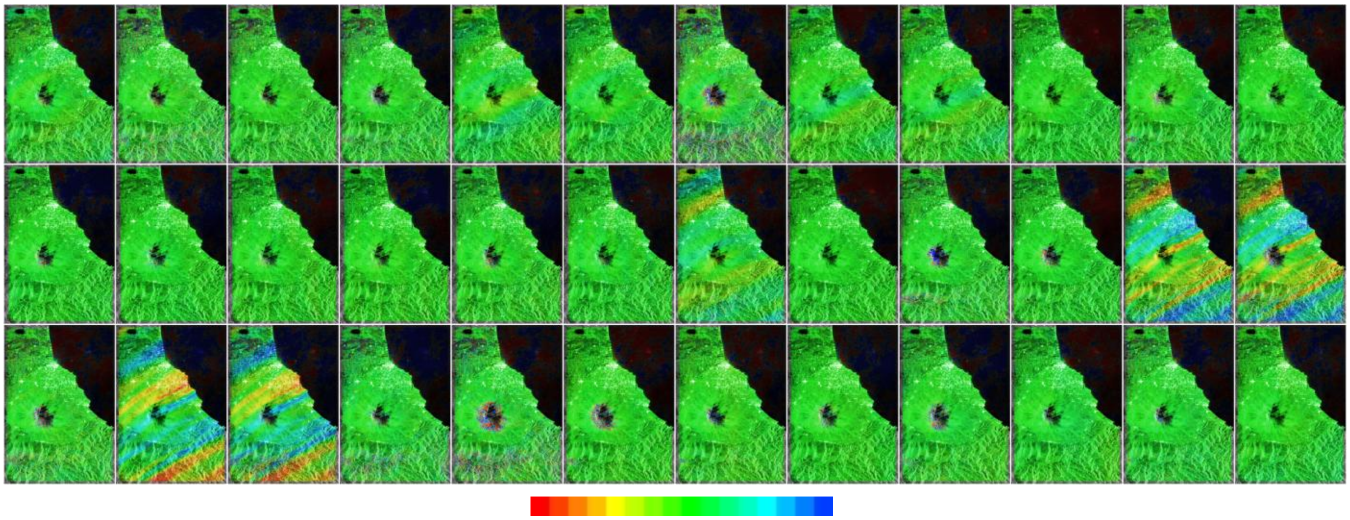

Figure 3 Multi-reference stack of PALSAR split-beam interferograms over the Etna volcano, Italy. The pairs shown are listed in Table 1. Very strong phase variations (ionospheric effects) are observed for the pairs 23,24,26,27 which all include the scene acquired on 19-Jun-2009. The images are shown in slant-range geometry.

Table 1: Dates of split-beam interferogram pairs of Figure 3.

No.	PALSAR pair	No.	PALSAR pair
1	20070127 20070614	19	20080616 20080916
2	20070127 20080916	20	20080916 20081101
3	20070127 20081101	21	20080916 20090201
4	20070127 20090201	22	20081101 20090201
5	20070614 20070730	23	20081101 20090619
6	20070614 20070914	24	20090201 20090619
7	20070614 20090201	25	20090201 20090804
8	20070730 20070914	26	20090619 20090804
9	20070730 20071030	27	20090619 20091220
10	20070914 20071030	28	20090804 20091220
11	20070914 20071215	29	20090804 20100204
12	20071030 20071215	30	20091220 20100204
13	20071030 20080130	31	20091220 20100322
14	20071215 20080130	32	20100204 20100322
15	20071215 20080316	33	20100204 20100507
16	20080130 20080316	34	20100322 20100507
17	20080130 20080501	35	20100322 20100807
18	20080316 20080501	36	20100507 20100807

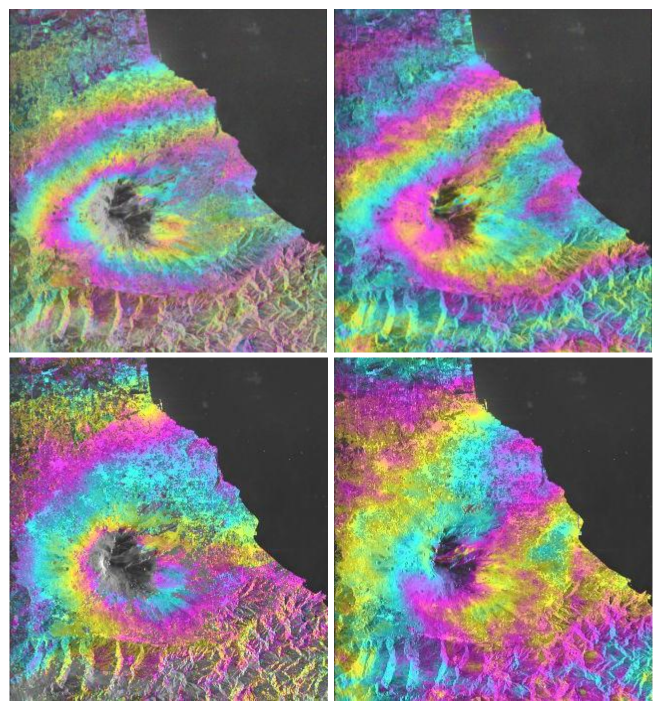

Figure 4 Two PALSAR differential interferograms (top) including the scene on 19-Jun-2009 over the Etna and corresponding "ionospheric delay corrected" interferograms (bottom). A color cycle corresponds to a phase cycle.

We integrated the split-beam interferograms in the azimuth direction to derive ionospheric path delay corrections for the corresponding interferograms. Examples of uncorrected and corrected differential interferograms that include the PALSAR scene on 19-Jun-2009 are shown in Figure 4. The corrected differential interferograms clearly show less phase variations. It is also obvious that the corrections do not perfectly flatten the differential interferograms. Partly, this is because of other phase terms such as the atmospheric path delay, the deformation phase, as well as residual orbital phase, residual topographic phase and phase noise, and partly due to the assumptions used in the determination of the integration constants used.

Using Singular Value Decomposition (SVD) we obtained then the least-squares solution for the phase time-series. Redundancy in the differential interferogram input data reduces uncorrelated errors in the time-series. Uncorrelated errors include residual topographic phase errors and phase noise. Atmospheric and ionospheric path delay phase on the other hand is not reduced by this estimation procedure. For a given acquisition date there is a well defined atmospheric and ionospheric phase delay pattern which is present in all the pairs including this date. The same applies for non-uniform deformation phase. Consequently, the obtained time series of unwrapped phases still includes the atmospheric and ionospheric phases as well as non-uniform deformation phase. Apart from the phase time series the RMS deviation of the values from the SVD is calculated as a quality measure, permitting to identify unwrapping errors which remained undetected.

To discriminate deformation on one hand and atmospheric and ionospheric path delay phase on the other hand we conducted a temporal analysis of the time series. The temporally correlated component was assigned as deformation phase, the uncorrelated phase as atmospheric and ionospheric phase. Applying linear regressions to the time series we estimated also linear deformation rates (Figure 5).

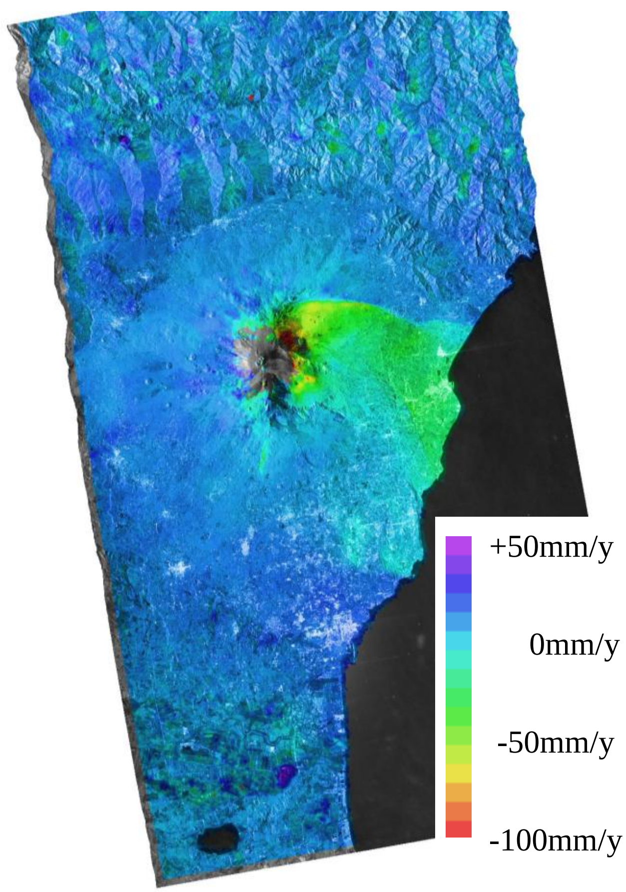

Figure 5 Linear deformation rate derived using 19 PALSAR scenes between 20070127 and 20100322.

4. CONCLUSIONS

The identification of ionospheric path delay effects using split-beam interferograms appears to be straight-forward, quite efficient, and reliable, as long as the pairs considered are sufficiently coherent. Such a test can be applied routinely in L-band interferometry and the processing sequence can be simplified using a co-registration procedure that does not consider ionosphere related azimuth offsets. Thanks to such testing the interpretation of the differential interferometric phase becomes more reliable.

The two main difficulties in the correction of ionospheric path delay effects based on the split-beam interferogram are the presence of gaps in the split-beam interferogram due to low coherence and the determination of the integration constant for the azimuth integrations. In practice small spatial gaps in the ionospheric path delay estimate can be filled by interpolation given its relatively low spatial variability.

The presented methodology also permits distinguishing ionospheric and tropospheric path delays. The reason is that the ionospheric path delay occurs at elevations around 300km which is a significant fraction of the satellite orbit elevation while the tropospheric path delay is located in the lowest few kilometers above the surface.

And finally, this methodology is also of interest for estimating the spatial variation in the ionospheric electron concentration [2].

5. ACKNOWLEDGEMENTS

This work is supported by the ESA DUE Project Permafrost. JAXA is acknowledged for the PALSAR data (AO 094).

6. REFERENCES

[1] Meyer F., R. Bamler, N. Jakowski, and T. Fritz, The potential of broadband L-band SAR systems for small scale ionospheric TEC mapping, Procs. FRINGE 2005 Workshop, Frascati, Italy, 28. Nov. - 2 Dec., 2005 (http://earth.esa.int/workshops/fringe2005).

[2] Wegmüller U., C. Werner, T. Strozzi, and A. Wiesmann, "Ionospheric electron concentration effects on SAR and INSAR", Proc. IGARSS 2006, Denver, Colorado, USA, 31- Jul. – 4. Aug. 2006.

[3] Bechor N. and H. Zebker, Measuring two-dimensional movements using a single InSAR pair, GRL Vol. 33, L16311, 2006.

[4] Wegmüller U., C. Werner, and R. Cordey, "Flashing fields! A preliminary investigation", Proc. ENVISAT Symposium 2004, Salzburg, Austria, 6-10 Sep. 2004.

[5] Wegmüller U., M. Santoro, C. Werner, T. Strozzi and A. Wiesmann, ERS-ENVISAT Tandem Cross-Interferometry Coherence estimation, Proc. IGARSS'09, Cape Town, South Africa, 13-17 Jul. 2009.